1 **Research article**

2 **Full title: GluD1 knockout mice with a pure C57BL/6N background**

3 **show impaired fear memory, social interaction, and enhanced**

4 **depressive-like behavior**

5

6 **Short title: Behavioral and biochemical analyses of GluD1 knockout**

7 **mice with a pure C57BL/6N background**

8

9 Chihiro Nakamoto[1,2,3], Meiko Kawamura[1], Ena Nakatsukasa[1], Rie Natsume[1], Keizo

10 Takao[4,5], Masahiko Watanabe[6], Manabu Abe[1*], Tomonori Takeuchi[2,3*], Kenji Sakimura[1]

11

12 **1** Department of Animal Model Development, Brain Research Institute, Niigata

13 University, Niigata, Japan

14 **2** Department of Biomedicine, Aarhus University, Aarhus, Denmark

15 **3** Danish Research Institute of Translational Neuroscience – DANDRITE, Nordic-EMBL

16 Partnership for Molecular Medicine, Aarhus University, Aarhus, Denmark

17 **4** Graduate School of Innovative Life Science, University of Toyama, Toyama, Japan

18 **5** Life Science Research Center, University of Toyama, Toyama, Japan

19 **6** Department of Anatomy, Faculty of Medicine, Hokkaido University, Sapporo, Japan

20

21 [*]Corresponding authors: tomonori.takeuchi@biomed.au.dk (T. Takeuchi) and

22 manabu@bri.niigata-u.ac.jp (M. Abe).

Abstract

The GluD1 gene is associated with susceptibility for schizophrenia, autism, depression, and bipolar disorder. However, the function of GluD1 and how it is involved in these conditions remain elusive. In this study, we generated a GluD1-knockout (GluD1-KO) mouse line with a pure C57BL/6N genetic background and performed several behavioral analyses. Compared to a control group, GluD1-KO mice showed no significant anxiety-related behavioral differences, evaluated using behavior in an open field, elevated plus maze, a light-dark transition test, the resident-intruder test of aggression and sensorimotor gating evaluated by the prepulse inhibition test. However, GluD1-KO mice showed (1) hyper locomotor activity in the open field, (2) decreased sociability and social novelty preference in the three-chambered social interaction test, (3) impaired memory in contextual, but not cued fear conditioning tests, and (4) enhanced depressive-like behavior in a forced swim test. Pharmacological studies revealed that enhanced depressive-like behavior in GluD1-KO mice was restored by the serotonin reuptake inhibitors imipramine and fluoxetine, but not the norepinephrine transporter inhibitor desipramine. In addition, biochemical analysis revealed no significant difference in protein expression levels, such as other glutamate receptors in the synaptosome and postsynaptic densities prepared from the frontal cortex and the hippocampus. These results suggest that GluD1 plays critical roles in fear memory, sociability, and depressive-like behavior.

Introduction

46

47 The δ-type ionotropic glutamate receptor consists of GluD1 (GluRδ1) and GluD2

48 (GluRδ2) [1–3]. Despite having conserved membrane topology and amino acid residues

49 critical for glutamate binding and Ca^{2+} permeability, the δ subfamily members do not

50 function as conventional glutamate-gated receptor channels when expressed alone or in

51 combinations with other ionotropic glutamate receptor subunits [4–6]. Instead, they are

52 components of a tripartite transsynaptic adhesion system, where the extracellular domain

53 of postsynaptic GluD1/2 interacts with that of presynaptic neurexin protein (NRXN) via

54 members of the cerebellin precursor protein (CBLN) family in the synaptic cleft [7–9].

55 Moreover, slow activity of GluD1/2 ion channels is triggered by activation of group 1

56 metabotropic glutamate receptors (mGluRs) [10–12].

57 GluD2 has been intensively studied since it was cloned in 1993 [2,3]. In the rodent

58 cerebellum, GluD2 is exclusively expressed in Purkinje cells and is selectively localized

59 to postsynaptic spines at parallel fiber synapses [13,14]. GluD2 is indispensable during

60 the formation and maintenance of parallel fiber-Purkinje cell synapses by interaction with

61 presynaptic neurexins through its amino-terminal domain [7,8,15,16]. In addition, GluD2

62 regulates cerebellar synaptic plasticity [15,17] and motor learning [15,18,19] by

63 interaction with the scaffolding proteins through its carboxyl-terminal domain [20–22].

64 The gene encoding GluD1 in humans (*GRID1*) is associated with a susceptibility

65 for schizophrenia [23–26], major depressive disorder [27], and autism spectrum disorder

66 [28–31]. GluD1 is expressed in various brain regions in rodents, including the cerebral

67 cortex, hippocampus, amygdala, bed nucleus of the stria terminalis, striatum, thalamus,

68 nucleus accumbens, lateral habenular, and the dorsal raphe nucleus [3,32,33]. Similar to

69   GluD2, postsynaptic GluD1 is required for synapse formation and maintenance *in vitro*

70   via CBLN1/CBLN2 and presynaptic NRXN [7,9,34,35]. In addition, GluD1 regulates

71   group 1 mGluRs-mediated long-term depression in the hippocampus *ex vivo* [36].

72   Furthermore, activation of group 1 mGluRs trigger the opening of GluD1 channels,

73   which are key determinants of the slow excitatory postsynaptic current *ex vivo* [12].

74   The GluD1 knockout (GluD1-KO) mice line (*Grid1*^{tm1Jnz}), compared to the

75   relevant control groups, showed abnormal behavioral phenotypes, such as hyper

76   locomotor activity, lower anxiety-like behavior, hyper aggression, higher depression-like

77   behavior, deficits in social interaction [37], enhanced working memory, deficit in

78   contextual and cued fear conditioning [38], and increased stereotyped behavior [39].

79   However, the *Grid1*^{tm1Jnz} mouse was generated from embryonic stem (ES) cells

80   derived from the 129/SvEv strain, followed by backcrossing to C57BL/6 mice 2–6

81   times [37,38,40]. It is well known that backcrossing with different mouse strains leads

82   to a change in the basal levels of behaviors, such as anxiety [41–43], aggression [44,45],

83   prepulse inhibition [46], social interaction [47,48], pain sensitivity [49], depressive-like

84   behavior [42,50–52], and learning and memory [41,53–56]. Thus, a concern of using a

85   mixed genetic background is that the resulting phenotype cannot be confidently

86   attributed to either the target gene or closely-linked genes flanking the targeted locus

87   [53,57,58]. In addition, the 129S6/SvEvTac strain used in *Grid1*^{tm1Jnz} lacked the

88   DISC1 gene (disrupted in schizophrenia 1) [59–61], which is a strong candidate gene

89   that contributes to cause schizophrenia and autism spectrum disorder [62,63]. Moreover,

90   the *Grid1*^{tm1Jnz} mouse was generated by knock-in of a selection marker of neomycin

91 cassette; the promoter of the cassette unexpectedly affected gene expression levels

92 [64–67].

93   To avoid these issues, we generated GluD1-KO mice with a pure C57BL/6N

94 genetic background and investigated an impact of GluD1 deletion on various behaviors

95 including anxiety, aggression, sensorimotor gating, sociability, learning and memory,

96 and depression.

97

Methods

98

Animals

99

100 GluD1-KO mice were generated using the C57BL/6N ES cell line, RENKA [65] and

101 maintained in a pure C57BL/6N background [68]. Briefly, exon 4 of the *Grid1* gene and

102 a *Pgk* promoter-driven neomycin-resistance cassette were flanked by loxP sequences

103 (*Grid1*$^{\text{flox}}$). *Grid1*$^{\text{flox}}$ mice were crossed with telencephalin-Cre mice [69] to create the

104 null allele (*Grid1*$^-$). Mice were fed *ad libitum* with standard laboratory chow and water

105 in standard animal cages in a 12-h light/dark cycle (light on at 8:00 a.m.) at room

106 temperature and relative humidity in the ranges of 22°C–24°C and 30%–70%,

107 respectively. Experimental protocols used throughout the study were approved by an

108 institutional committee at Niigata University (SA00466) and were in accord with

109 Japanese legislation concerning animal experiments.

110   Behavioral tests were carried out with 8 to 12-week-old male wild-type (WT,

111 *Grid1*$^{+/+}$) (n = 115 in total) and GluD1-KO (*Grid1*$^{-/-}$) (n = 92 in total) litter mates by

112 heterozygous breeding, and were performed during the light phase (between 10:00 a.m.

113 and 18:00 p.m.). Mice were handled (3 min per day for 3 days) before starting

114 behavioral tests. Behavioral analyses were performed with the experimenter blind to

115 mice genotype. After each trial, the apparatus was cleaned with hypochlorous water to

116 prevent a bias due to olfactory cues. A battery of behavioral tests were performed in the

117 following order: open field, light-dark transition, elevated plus maze, 3-chamber social

118 interaction, and a forced swim.

119

Open field

121 Open field tests were carried out using a method similar to that reported previously,

122 with minor modification [70]. Each mouse was placed in the corner of an open field

123 apparatus (50 cm × 50 cm × 40 cm high; O'Hara & Co., Tokyo, Japan) with a chamber

124 illuminated at either 5 or 100 lux. Distance traveled and time spent in the central area

125 (defined as 25% of total area) were recorded and calculated automatically over a 10-min

126 period using Image OFCR software (O'Hara & Co.; see 'Image analysis for behavioral

127 tests').

128

Elevated plus maze

130 Elevated plus maze tests were carried out using a method similar to that reported

131 previously, with minor modification [70]. The apparatus consisted of two open arms (25

132 cm × 5 cm) and two enclosed arms of the same size with transparent walls (height 15

133 cm). The arms and central square (5 cm × 5 cm) were made of white plastic plates and

134 were elevated 60 cm above the floor (O'Hara & Co.). Arms of the same type were

135 oriented opposite from each other. Each mouse was placed in the central square of the

136   maze, facing one of the closed arms. The time spent in closed and open arms and the

137   frequency of entry into open arms were observed for 10 min under two different

138   illumination condition (5 and 100 lux). Data acquisition was performed automatically

139   using Image EP software (O'Hara & Co.; see 'Image analysis for behavioral tests').

140

Light-dark transition test

141

142   Light-dark transition tests were carried out using a method similar to that reported

143   previously, with minor modification [70]. The apparatus consisted of a cage (21 cm ×

144   42 cm × 25 cm high) divided into 2 equal chambers by a black partition containing a

145   small opening (5 cm x 3 cm high) (O'Hara & Co.). One chamber was made of white

146   plastic and was brightly illuminated (252 lux), whereas the other chamber was made of

147   black plastic and was dark (no illumination). Mice were placed in the dark chamber and

148   allowed to move freely between the two chambers for 10 min. Time spent in each

149   chamber, total number of transitions and latency to the first transition from dark to light

150   chambers were recorded automatically using Image LD software (O'Hara & Co.; see

151   'Image analysis for behavioral tests').

152

Resident-intruder test

153

154   Resident-intruder tests were carried out using a method similar to that reported

155   previously [37]. Resident male WT (27.3 ± 0.2 g) or GluD1-KO mice (24.1 ± 0.4 g)

156   were individually housed for 3-4 weeks before testing. Resident mice were exposed to

157   intruder male WT C57BL/6 mice, which had been group-housed (four to five per cage)

158   and were of lower body-weight than resident mice (0-4 g lighter than intruder mice), for

159   a duration of 10 min. New intruder mice were used in each test. Latency to attack the

160   intruder and attack frequency were measured manually.

161

Prepulse inhibition test

163   Acoustic startle response and prepulse inhibition (PPI) of the acoustic startle response

164   were measured using a startle chamber (SR-Lab Systems; San Diego Instruments, CA,

165   USA)[71]. For acoustic startle responses, a background of white noise was used (70 db).

166   An animal was placed in the Plexiglass cylinder and each test session began after 5 min

167   of acclimatization. Mice were presented with 64 trials. There were eight different sound

168   levels presented: 75, 80, 85, 90, 95, 100, 110, and 120 dB. Each white-noise stimulus

169   was 40 ms and presented 8 times in a pseudorandom order such that each sound level

170   was presented within a block of 8 trials. The intertrial interval was 15 s. Analysis for

171   startle amplitudes was based on the mean of the seven trials (ignoring the first trial) for

172   each trial type.

173   PPI responses were measured with acoustic stimuli (120 dB) combined with four

174   different prepulse intensities. Each mouse was placed in the startle chamber and initially

175   acclimatized for 5 min with background white noise alone (70 dB). Mice were then

176   presented with 48 trials. Each session consisted of six trial types. One trial type used a

177   sound burst (40 ms, 120 dB) as the startle stimulus (startle trials). There were four

178   different trials consisting of acoustic prepulse and acoustic startle stimuli (prepulse

179   trials). The prepulse stimulus (20 ms) of either 73, 76, 79, or 82 dB was presented 100

180   ms before the onset of the acoustic startle stimulus. Finally, there were trials where no

181   stimulus was presented (no-stimulus trials). The six trial types were presented in a

182   pseudorandom order such that each trial type was presented once within a block of eight

183 trials. The intertrial interval was 15 s. Analysis was based on the mean of the seven

184 trials (ignoring the first trial) for each trial type. The percentage PPI of a startle response

185 was calculated using the following equation: $100 - [100 \times$ (startle response on prepulse

186 trials − no stimulus trials)/(startle trials − no stimulus trials)].

187

Three-chambered social interaction test

189 The three-chambered social interaction test was performed as previously described, with

190 minor modification [48,70]. The apparatus consisted of a rectangular, illuminated (5

191 lux) three-chambered box with a lid and an attached infrared video camera (O'Hara &

192 Co.). Each chamber was 20 cm × 40 cm × 22 cm (high) and the dividing walls were

193 made of clear Plexiglas, with small square openings (5 cm wide × 3 cm high) to allow

194 exploration of each chamber. Male mice of the C3H strain, with ages ranging between 8

195 to 12 weeks, were purchased from Charles River Laboratories (Yokohama, Japan) and

196 used as 'strangers'.

197 One day before testing, the 'subject mice' were individually placed in the middle

198 chamber and allowed to freely explore the entire apparatus for 5 min. Before testing,

199 subject mice were placed in the middle chamber and allowed to freely explore all three

200 chambers for 10 min (habituation trial). In the sociability test (sociability trial), an

201 unfamiliar C3H male mouse ('stranger 1') that had no prior contact with the subject

202 mouse was placed in one of the side chambers. The stranger mouse was enclosed in a

203 small, round wire cage, which allowed nose contact between the bars but prevented

204 fighting. This cage was 11 cm in height, with a floor diameter of 9 cm and vertical bars

205 0.5 cm apart. The subject mouse was placed in the middle chamber and presented with

206 stranger 1 in one compartment and an empty cage in another compartment for 10 min.

207   The amount of time spent around each cage (stranger 1 or empty) was measured. At the

208   end of the 10-min sociability trial, each subject mouse was then tested in a 10-min trial

209   to quantitate social preference for a new stranger (social novelty preference trial). The

210   wire cage enclosing the familiar C3H male mouse (stranger 1) was moved to the

211   opposite side of the chamber that had been empty during the sociability trial. A second,

212   unfamiliar C3H male mouse (stranger 2) was placed in the other side of the chamber in

213   an identical small wire cage. The subject mouse was free to explore the mouse from the

214   previous sociability test (stranger 1), and the novel mouse (stranger 2). The amount of

215   time spent around each cage (stranger 1 or stranger 2) was measured. Data acquisition

216   and analysis were performed automatically using Image CSI software (O'Hara & Co.;

217   see 'Image analysis for behavioral tests').

218

Contextual and cued fear conditioning test

220   The contextual and cued fear conditioning test was performed using a method similar to

221   a previous report [70], with minor modifications. Fear conditioning was conducted in a

222   transparent acrylic chamber (33 cm□×□25 cm□×□28 cm high) with a stainless-steel

223   grid floor (0.2 cm-dimeter, spaced 0.5 cm apart; O'Hara & Co.). For the conditioning

224   (conditioning test), each mouse was placed in the chamber and was allowed to explore

225   freely for 3 min. Subsequently, white noise (55 dB) was played through a speaker set on

226   top of the conditioning chamber wall, which served as the conditioning stimulus (CS),

227   was presented for 20 s. During the last 2 s of CS presentation, mice received a

228   footshock (0.7 mA, 2 s), which served as an unconditioned stimulus (US). Two more

229   CS-US pairings were presented with a inter-stimulus interval of 40 s. Animals were

230   returned to their home cages 40 s after the last CS-US paring. Twenty-four hours after

231 conditioning (contextual test), contextual fear memory was tested for 3 min in the same

232 chamber. Forty-eight hours after conditioning (cued test), cued fear memory was tested

233 with an altered context. Each mouse was placed in a triangular chamber (33 cm ×33

234 cm ×32 cm high) made of opaque white plastic and allowed to explore freely for 1

235 min. Subsequently, each mouse was given CS presentation for 3 min. In each session,

236 percentage of time spent freezing was calculated automatically using Image FZ software

237 (O'Hara & Co.; see 'Image analysis for behavioral tests').

238 Pain sensitivity was measured as a control experiment using the fear conditioning

239 chamber apparatus in a manner similar to a previous study [38]. Following 2 min of

240 habituation, mice were given footshocks of increasing strength ranging from 0.05 to 0.7

241 mA in a stepwise manner by 0.05 mA, with an intertrial interval of 30 s. We measured

242 current thresholds for three reactions of mice to nociceptive shock: flinch, vocalization,

243 and jump (vertical and horizontal). Scoring indicated the first shock intensity at which

244 each pain reaction was detected.

245

Forced swim test with pharmacological manipulation

247 Forced swim tests were performed following Porsolt's method with minor

248 modifications [37,72]. The apparatus consisted of a transparent plastic cylinder (22 cm

249 height; 12 cm diameter) placed in a box (41 cm × 31 cm × 42 cm high; O'Hara & Co).

250 The cylinder was filled with water (22 ± 1°C) up to a height of 10 cm. Each mouse was

251 placed into the cylinder and activity was monitored for 5 min via a CCD camera

252 mounted on the top of the box. The cylinder was refilled with clean water after each test.

253 Image data acquisition and analysis were performed automatically using Image PS

254 software (see 'Image analysis for behavioral tests').

255   With respect to drugs, saline (0.9% NaCl in H_2O) was used as a vehicle and for

256   control injections. Drug concentration for injections were: 15 mg/kg of imipramine

257   (097-06491; FUJIFILM Wako Pure Chemical Corporation, Osaka, Japan), 10 mg/kg of

258   fluoxetine (F132; Sigma-Aldrich, MO, USA), 30 mg/kg of desipramine (042-33931;

259   FUJIFILM Wako Pure Chemical Corporation). Drug concentrations were chosen on the

260   basis of previous studies for imipramine [52][73][74][75][76], fluoxetine

261   [52][73][77][76], and desipramine[52][73][74][76][78]. Both vehicle and drug solutions

262   were intraperitoneally administered. Sixty min after injection, mice were tested in the

263   open field for 10 min with 5 lux illumination and subsequently subjected to a forced swim

264   test for 5 min.

265

Image analysis for behavioral tests

267   The application software used for the behavioral studies (Image OFCR, LD, EP, CSI,

268   PS, and FZ) were based on the public domain NIH Image program (developed at the

269   U.S. National Institutes of Health and available at http://rsb.info.nih.gov/nih-image/)

270   and ImageJ program (http://rsb.info.nih.gov/ij/), which were modified for each test

271   (available through O'Hara & Co.).

272

Subcellular fraction and western blot analysis

274   Subcellular fractions were prepared following Carlin's method [79] with minor

275   modifications. All processes were carried out at 4 °C. Briefly, WT and GluD1-KO mice

276   with a C57BL/6N background (8 to 12 weeks old) were decapitated after cervical

277   dislocation, and the frontal cortex (defined as one third anterior part of the cerebral

278   cortex) and hippocampus were immediately dissected and removed. Brain tissues were

279   homogenized in homogenization buffer [320 mM sucrose and 5 mM EDTA, containing

280   complete protease inhibitor cocktail tablet (Complete Mini; Roche, Mannheim,

281   Germany)] and centrifuged at $1,000 \times g$ for 10 min. The supernatant was centrifuged at

282   $12,000 \times g$ for 10 min, and the resultant pellet was re-suspended in homogenization

283   buffer as the P2 fraction. The P2 fraction was layered over a 1.2 M/0.8 M sucrose

284   gradient and centrifuged at $90,000 \times g$ for 2 h. The synaptosome fraction was collected

285   from the interface, mixed with equal volume of Triton solution [1% Triton X-100, 0.32

286   M sucrose, 12 mM Tris-Cl (pH 8.0)] for 15 min, and centrifuged at $200,000 \times g$ for 1 h.

287   The resultant pellet was suspended in 40 mM Tris-Cl (pH 8.0), 1% SDS as the post

288   synaptic density (PSD) fraction. The protein concentration was determined using BCA

289   Protein Assay Reagent (Thermo Fisher Scientific, MA, USA). Equal volume of SDS

290   sample buffer [125 mM Tris-Cl (pH 6.8), 4% SDS, 20% glycerol, 0.002% BPB, 2%

291   2-mercaptoethanol] was added to the sample fractions and boiled for 5 min at 100 °C.

292   Protein samples were separated by 8% SDS-PAGE and electrophoretically

293   transferred to nitrocellulose membranes (GE Healthcare, NJ, USA). Both WT and

294   GluD1-KO mice samples were blotted on the same membrane for quantification.

295   Membranes were blocked with 5% skimmed milk in TBS-T [20 mM Tris-Cl (pH 7.6),

296   137 mM NaCl, 0.1% Tween 20] for 1 h, and incubated with each primary antibody (1

297   μg/ml) (Table 1) for 3-4 h and horseradish peroxidase-conjugated secondary antibody

298   for 1 h. Between these incubation steps, membranes were washed three times with

299   TBS-T for 30 min. Protein bands were visualized with an enhanced chemiluminescence

300   (ECL) kit (GE Healthcare) using a luminescence image analyzer with an electronically

301   cooled charge-coupled device camera (EZ capture MG; ATTO, Tokyo, Japan). Signal

302 intensities of immunoreacted bands were determined using CS Analyzer ver.3.0

303 (ATTO).

304

305 **Table 1.** Primary antibodies used in the present study

306

	Sequence (NCBI #)	RRID	Host	Specificity	Reference/Source
GluA1	841-907 aa (X57497)	AB_2571752	Rb	KO	FI (GluA1-Rb-Af690)
GluA1	880-907 aa	n/a	Rb	IB	[80]
GluA2	175-430 aa (NM_013540)	AB_2113875	Ms		Millipore (MAB397)
GluN2A	1126-1408 aa	AB_2571605	Rb	KO	[81] FI (GluRe1C-Rb-Af542)
GluN2B	1301-1456 aa (D10651)	AB_2571762	Rb	KO	FI(GluRe2C-Rb-Af300)
GluK2	844-908 aa (P42269)	n/a	Rb	KO	[82] Synaptic systems (180 003)
GluD1	895-932 aa (NM_008166)	AB_2571757	Rb	KO	[32] FI (GluD1C-Rb-Af1390)
GluD2	897-934 aa (D13266)	AB_2571601	Rb	KO	[68]
PSD-95	1-64 aa (D50621)	AB_2571611	Rb	IB	[83] FI (PSD-95-Rb-Af1720)

307

308 aa, amino acid residues; FI, Frontier Institute; GluA1, AMPA-type glutamate receptor-1;

309 GluA2, AMPA-type glutamate receptor-2; GluD1, delta-type glutamate receptor-1;

310 GluD2, delta-type glutamate receptor-2; GluK2, kainate-type glutamate receptor-2;

311 GluN2A, N-methyl-D-aspartate glutamate receptor-2A; GluN2B, N-methyl-D-aspartate

312 glutamate receptor-2B; GP, guinea pig polyclonal antibody; KO, lack of

14

313   immunohistochemical or immunoblot labeling in knockout mice; Ms, mouse monoclonal

314   antibody; Rb, rabbit polyclonal antibody; RRID, Research Resource Identifier.

315

Statistical analysis

317   All data are expressed as mean ± SEM. Statistical analyses for behavioral studies were

318   performed using EZR (Saitama Medical Center, Jichi Medical University, Saitama,

319   Japan), which is a graphical user interface for R (The R Foundation for Statistical

320   Computing, Vienna, Austria). Data were analyzed by one-way ANOVA, two-way

321   ANOVA, two-way repeated-measures ANOVA followed by Dunnett's post hoc tests, or

322   Student's t-test with Welch's correction as appropriate to correct for multiple

323   comparisons. Attack latency in the resident-intruder test was analyzed using

324   Kaplan-Meier survival curves followed by Mantel-Cox log-rank tests. All statistical

325   tests were two-tailed. The level of significance set was $p < 0.05$.

326

Results

Normal anxiety-related behavior in GluD1-KO mice

329   To determine whether GluD1 was involved in anxiety-related behavior, we performed

330   tests in an open field (Fig 1A), an elevated plus maze (Fig 1F), and a light-dark transition

331   test (Fig 1M). It is well established that performance in both the open field and elevated

332   plus maze are influenced by the arena illumination levels [84,85]. We therefore used two

333   different illumination conditions (5 and 100 lux) in these tests.

334

335 **Fig 1. Hyperlocomotor activity but normal anxiety-related behavior in GluD1-KO**

336 **mice.** (A-E) The open field. Schematic representation of the open field test (A).

337 GluD1-KO mice traveled significantly longer than WT in the open field test with 5 lux

338 illumination (WT, n = 19; GluD1-KO, n = 13; p < 0.05, unpaired Student's t-test) (B), and

339 100 lux (WT, n = 33; GluD1-KO, n = 24; p < 0.05) (D). No significant difference was

340 observed in the time spent in the central region with 5 lux (p = 0.46) (C) or 100 lux (p =

341 0.08) illumination (E). (F-L) The elevated plus maze. Schematic representation of the

342 elevated plus maze (F). There were no significant differences between WT (5 lux, n = 16;

343 100 lux, n = 21) and GluD1-KO mice (5 lux, n = 10; 100 lux, n = 19) in the time spent in

344 the closed arms [5 lux, p = 0.87 (G); 100 lux, p = 0.25 (J)] or in the open arms [5 lux, p =

345 0.95 (H); 100 lux, p = 0.72 (K)], or in the number of entries into the open arms [5 lux, p =

346 0.92 (I); 100 lux, p = 0.70 (L)]. (M-P) The light-dark transition test. Schematic

347 representation of the light-dark transition test (M). There was no significant difference

348 between WT (n = 33) and GluD1-KO mice (n = 23) in the time spent in the dark and light

349 boxes [Dark box, p = 0.62; Light box, p = 0.62 (N)], in the number of entries into the light

350 box (p = 0.85) (O), or in latency to first transition into the light box (p = 0.17) (P). *p <

351 0.05, unpaired Student's *t*-test with Welch'correction. All values presented are mean ±

352 SEM.

353

354 We performed the open field test for a total duration of 10 min (Fig 1A). The open

355 field test presents a conflict between innate drives to explore a novel environment and

356 personal safety [86]. GluD1-KO mice traveled longer distances compared to WT mice

357 under both illumination conditions (Fig 1B, D). We also calculated the percentage of time

358 spent in the central area of the open field, which is commonly used as an index of anxiety

359   [41]. There were no significant differences in the percentage of time spent in the central

360   area between WT and GluD1-KO mice under either illumination conditions (Fig 1C, E).

361   In the elevated plus maze, we did not detect any significant differences in the time

362   spent in the closed or open arms between genotypes, or in the number of entries into the

363   open arm between genotypes under either of the illumination conditions (Fig 1G–L).

364   There was no significant differences between WT and GluD1-KO mice in total distance

365   traveled using 5 lux (WT, 15.6 ± 1.0 meters; GluD1-KO, 18.3 ± 0.96 meters; $p = 0.076$)

366   or 100 lux (WT, 19.5 ± 0.96 meters; GluD1-KO, 21.7 ± 1.1 meters; $p = 0.142$) and no

367   differences in total entries using 5 lux (WT, 26 ± 2.4; GluD1-KO, 30 ± 2.8; $p = 0.256$) or

368   100 lux (WT, 34 ± 2.0; GluD1-KO, 39 ± 2.4; $p = 0.162$).

369   Besides, we performed another behavioral assay for studying anxiety in mice, the

370   light-dark transition test (Fig 1M). There was no significant difference between WT and

371   GluD1-KO mice in the time spent in the light and dark portions of the box (Fig 1N), in

372   transition number between the illuminated and dark areas (Fig 1O), or in latency to enter

373   the illuminated area of the box (Fig 1P).

374   Together, GluD1-KO mice showed hyper-locomotor activity in the open field test;

375   however, GluD1-KO mice did not show any anxiety-related behaviors in the open field,

376   elevated plus maze, or light-dark transition tests.

377

Normal aggression-like behavior in GluD1-KO mice

379   GluD1-KO mice were rare to show aggressive-like behavior in their home cage. In

380   accordance with these observations, both latency to attack first and attack frequency in

381   GluD1-KO mice were not significantly different from that of WT mice in the

382   resident-intruder test (Fig 2).

383

384 **Fig 2. Normal aggression-like behavior in GluD1-KO mice.** In the resident-intruder

385 test, there was no significant difference between WT (n = 8) and GluD1-KO (n = 7)

386 mice in attack latency (left; log-rank test, χ^2 = 2.451, p = 0.117) or attack frequency

387 (right, unpaired student's t-test, p = 0.304). All values presented are mean ± SEM.

388

Normal sensorimotor gating in GluD1-KO mice

390 Because human mutations of the *Grid1* gene are associated with schizophrenia [23–25],

391 we next performed PPI of the acoustic startle response, which is one of the most

392 promising electrophysiological endophenotypes of both patients and animal models of

393 schizophrenia [87–90]. In the acoustic startle responses, the amplitude of startle

394 responses was dependent on pulse intensity. There was no difference between genotypes

395 (Fig 3A).

396   We then examined PPI levels of WT and GluD1-KO mice using four different

397 prepulse intensities. Induction of PPI using 73-, 76-, 79- and 82-dB prepulse in the

398 120-dB startle condition occurred in both WT and GluD1-KO mice (Fig 3B). There was

399 no significant difference between WT and GluD1-KO mice in PPI levels, suggesting

400 normal sensorimotor gating in GluD1-KO mice.

401

402 **Fig 3. Normal startle response and prepulse inhibition in GluD1-KO mice.** (A)

403 Acoustic startle reflex test: Startle responses amplitudes were dependent on pulse

404 intensity (WT, n = 7; GluD1-KO, n = 9) (two-way ANOVA: $F_{7,112}$ = 24.2, p < 0.001).

405 There was no difference between genotype ($F_{1,112}$ = 0.08, p = 0.78), and no interaction

406 between genotype and tone intensity ($F_{7,112}$ = 0.13, p = 1.00). (B) Prepulse inhibition test:

407   The PPI levels of WT (n = 11) and GluD1-KO mice (n = 12) were not significantly

408   different with prepulses of 73, 76, 79 and 82 dB (two-way ANOVA: Genotype; $F_{1,84} =$

409   2.64, p = 0.11). PPI levels were dependent on prepulse intensity ($F_{3,84} = 18.09$, p < 0.001).

410   There was no significant interaction between genotype and prepulse intensity ($F_{3,84} = 0.08$,

411   p = 0.97). All values presented are mean ± SEM.

412

413   Social deficiency in GluD1-KO mice

414   We then examined the three-chamber social interaction test, which consists of a

415   sociability test and a social novelty preference test [48] (Fig 4). In the sociability test, a

416   wire cage with a stranger mouse (Stranger 1) was placed in one of the side chambers, and

417   an empty cage was placed in another side chamber (Fig 4A). The preference of the mouse

418   can be quantified based on the time spent around the wire cage with a stranger mouse

419   versus the empty cage. GluD1-KO mice spent a significantly shorter time around the wire

420   cage with the stranger mouse than that of WT mice (Fig 4B) indicating a lack of

421   sociability.

422   In the social novelty preference test, a second stranger mouse (Stranger 2) was

423   introduced into the empty cage. GluD1-KO mice spent a significantly shorter time around

424   the wire cage with the novel stranger mouse (stranger 2) than that of WT mice (Fig 4C)

425   indicating a lack of preference for social novelty.

426

427   **Fig 4. Reduced sociability and preference for social novelty in GluD1-KO mice.** (A)

428   Schematic representation of the three-chamber social interaction test. Sociability test

429   (middle): a wire cage with a stranger mouse (Stranger 1) was placed in one side chamber

430   and an empty wire cage was placed on the opposite side chamber. Social novelty

431 preference test (right): a novel stranger mouse (Stranger 2) was placed in a wire cage in

432 one side chamber and a familiar mouse (Stranger 1) was placed in a wire cage on the

433 opposite site. (B) Sociability test: there was a significantly lower time spent near the wire

434 cage with Stranger 1 in GluD1-KO (n = 23) than that of WT mice (n = 25) (p < 0.01). (C)

435 Social novelty preference test: there was significantly lower time spent near the wire cage

436 with stranger 2 in GluD1-KO mice than that of WT mice (p < 0.05). All values presented

437 are mean ± SEM. *p < 0.05; **p < 0.01, unpaired Student's t-test with Welch's

438 correction.

439

Impaired contextual fear memories in GluD1-KO mice

441 To assess the involvement of GluD1 in fear memory, we performed contextual and cued

442 fear conditioning tests (Fig 5). The freezing responses in the conditioning session did not

443 differ significantly between genotypes (Fig 5A). In the contextual test, GluD1-KO mice

444 exhibited a modest but significant decrease in the freezing response relative to WT mice

445 (Fig 5B).

446 In contrast, GluD1-KO mice showed no significant difference in freezing response

447 relative to WT mice in the cued test (Fig 5C). There were no significant differences in

448 pain sensitivity (Fig 5D) or hearing ability (Fig 3A) between genotypes, suggesting that

449 ablation of GluD1 caused deficits of contextual, but not cued memories in the fear

450 conditioning tests.

451

452 **Fig 5. Impaired contextual, but not cued memory in GluD1-KO mice in the fear**

453 **conditioning test.** (A) Schematic representation of the conditioning test (left). Freezing

454 responses on the conditioning test; there was no significant difference between WT (n =

455 8) and GluD1-KO (n = 9) mice (two-way repeated-measures ANOVA: Genotype; $F_{1,15} =$

456 0.0075, p = 0.93, US presentation; $F_{3,45} = 14.5$, p < 0.0001, Genotype × US presentation;

457 $F_{3,45} = 0.523$, p = 0.67). (B) Contextual test: freezing responses on the contextual testing

458 24 h after conditioning. There was significantly lower freezing in GluD1-KO mice during

459 contextual conditioning (p < 0.01, unpaired Student's t-test). (C) Cued test: freezing

460 responses on the cued testing 48 h after conditioning. There was no significant difference

461 between WT and GluD1-KO mice in cued conditioning during pre-tone and tone

462 (pre-tone, p = 0.62; tone, p = 0.14; unpaired Student's t-test). (D) Pain sensitivity test;

463 there were no significant differences between WT (n = 14) and GluD1-KO (n = 11)

464 mice in the footshock test evaluated by flinch (p=0.24), vocalization (p=0.24), vertical

465 jump (p=0.91) and horizontal jump (p=0.56). All values presented are mean ± SEM. **p

466 < 0.01.

467

468 Restoring depression-like behavior in GluD1-KO mice using a

469 serotonin transporter blocker

470 To analyze depression-like behavior, we used the Porsolt forced-swim test [72] (Fig 6).

471 GluD1-KO mice showed significantly increased immobility, indicating enhanced

472 depressive-like behavior (Fig 6A).

473

474 **Fig 6. Enhanced depressive-like behavior in GluD1-KO mice.** (A) Schematic

475 representation of the forced-swim test (left). There was significantly higher percentage

476 immobility in GluD1-KO mice (n = 22) than WT (n = 30) (middle) (two-way repeated

477 measures ANOVA: Genotype, $F_{1,50} = 5.66$, p < 0.05; Time, $F_{4,200} = 25.1$, p < 0.001;

478   Genotype × Time, $F_{4,200} = 1.56$, $p = 0.19$). Average immobility times for minutes 1 to 5 in

479   the forced-swim test (right). There was a significantly higher immobility in GluD1-KO

480   than WT mice ($p < 0.05$, unpaired Student's t-test). (B) Impact of antidepressants on the

481   forced-swim test. Animals were injected intraperitoneally with saline (WT, n = 12;

482   GluD1-KO, n = 8), imipramine (15 mg/kg) (WT, n = 12; GluD1-KO, n = 8), fluoxetine

483   (10 mg/kg) (WT, n = 11; GluD1-KO, n = 9), or desipramine (30 mg/kg) (WT, n = 9;

484   GluD1-KO, n = 9). Mice were subjected to open field test 60 min after injection for 10

485   min, and subsequently subjected to a forced-swim test for 5 min. Average immobility

486   times for 3 to 5 min: there was a significant genotype and treatment effect between and

487   WT and GluD1-KO mice (two-way ANOVA: Genotype, $F_{1,70} = 29.13$, $p < 0.001$; Drug,

488    $F_{3,70} = 6.16$, $p < 0.001$), but no significant interaction ($F_{3,70} = 2.56$, $p = 0.06$).

489   Within-genotype testing revealed that imipramine and fluoxetine led to a reduction in

490   immobility in GluD1-KO mice (one-way ANOVA with Dunnett's post hoc test: $F_{3,30} =$

491   5.58, $p = 0.004$; Imipramine, $p = 0.0017$; Fluoxetine, $p = 0.032$; Desipramine, $p = 0.42$).

492   In WT mice, no significant differences in immobility were observed with these

493   antidepressants ($F_{3,40} = 1.78$, $p = 0.17$; Imipramine, $p = 0.85$, Fluoxetine, $p = 0.74$;

494   Desipramine, $p = 0.41$). All values presented are mean ± SEM. *$p < 0.05$; **$p < 0.01$,

495   Dunnett's post hoc test. Desi, desipramine; Flu, fluoxetine; Imi, imipramine.

496

497   Next, we tested the impact of representative antidepressants on depression-like

498   behavior in GluD1-KO mice. Imipramine and fluoxetine are inhibitors of the serotonin

499   transporter, while desipramine is an inhibitor of the norepinephrine transporter. [91,92].

500   These drugs were injected intraperitoneally into WT or GluD1-KO mice 70 min before

501   the forced-swim test (Fig 6B). Before the forced-swim test, an open field test (10 min)

502   was conducted to confirm that these drugs did not produce false-positive results on

503   restoring depression-like behavior in the forced-swim test due to an increase of locomotor

504   activity.

505   Injection of imipramine and desipramine, but not fluoxetine led to a reduction in

506   the total distance in WT mice (One-way ANOVA with Dunnett's post hoc test: $F_{3,40} =$

507   6.41, p = 0.0012; Saline, 36.9 ± 2.3 meters; Imipramine, 25.5 ± 3.3 meters, p = 0.035;

508   Fluoxetine, 37.0 ± 1.4 meters, p = 1.0; Desipramine, 27.5 ± 1.9 meters, p = 0.032) in the

509   open field test). In contrast, no significant differences were observed in these

510   antidepressants in GluD1-KO mice ($F_{3,30}$ = 3.489, p = 0.028; Saline, 37.6 ± 2.0 meters;

511   Imipramine, 31.7 ± 2.2 meters, p = 0.10; Fluoxetine, 38.1 ± 1.6 meters, p = 1.0;

512   Desipramine, 31.8 ± 1.8 meters, p = 0.093).

513   In the forced-swim test, no significant differences were observed in these

514   antidepressants in WT mice, possibly due to a ceiling effect. Of note, differences in

515   percentage immobility for the saline-injected versus naïve WT mice in the forced-swim

516   test may have arisen due to injection stress. Injected of GluD1-KO mice with imipramine

517   and fluoxetine, inhibitors of the serotonin transporter, led to a reduction in percentage

518   immobility in the forced-swim test (Fig 6B). In contrast, a reduction in percentage

519   immobility was not observed with GluD1-KO mice with desipramine, an inhibitor of the

520   norepinephrine transporter (Fig 6B). These results suggest that inhibition of the serotonin

521   transporter, but not norepinephrine transporter, restored depression-like behavior in

522   GluD1-KO mice.

523

524 **Normal glutamate receptor levels and expression of PSD-95**

525 **protein in the frontal cortex and hippocampus of GluD1-KO**

526 **mice**

527 Finally, we measured levels of synaptic protein expression in GluD1-KO mice. We

528 analyzed the excitatory synaptic proteins, such as AMPA

529 (α-amino-3-hydroxy-5-methyl-4-isoxazole propionic acid)-type (GluA1 and GluA2),

530 NMDA (N-methyl-D-aspartate)-type (GluN2A and GluN2B), Kainite-type (GluK2), and

531 δ-type (GluD2) glutamate receptors and PSD-95 in the synaptosome and PSD fractions

532 prepared from the frontal cortex and the hippocampus. Inconsistent with previous reports

533 [38,39], we did not observe significant alterations of protein expression levels in any of

534 these proteins in both synaptosome (Fig 7A) and PSD fractions (Fig 7B) in GluD1-KO

535 mice. What did, however, find small but significant increases in expression of GluD2 in

536 the PSD fractions of both the frontal cortex and the hippocampus of GluD1-KO mice (Fig

537 7B).

538

539 **Fig 7. Normal protein expression in synaptosome and PSD fractions prepared from**

540 **the frontal cortex and the hippocampus of GluD1-KO mice.** (A) Protein expression

541 in synaptosome fractions prepared from the frontal cortex and hippocampus. The

542 protein loaded in lanes for GluA1, GluA2, GluN2A, GluN2B, GluK2, and PSD-95 were

543 20 μg, and 30 μg for GluD2. There was no significant difference between WT and

544 GluD1-KO mice in the protein expression prepared from the synaptosome fractions of

545 the frontal cortex (GluA1, $p = 0.59$; GluA2, $p = 0.89$; GluN2A, $p = 0.34$; GluN2B, $p = 0.33$; GluK2, $p = 0.73$; GluD2, $p = 0.27$; PSD-95, $p = 0.71$) and the hippocampus

546 0.33; GluK2, $p = 0.73$; GluD2, $p = 0.27$; PSD-95, $p = 0.71$) and the hippocampus

547   (GluA1, p = 0.59; GluA2, p = 0.60; GluN2A, p = 0.96; GluN2B, p = 0.46; GluK2, p =

548   0.86; GluD2, p = 0.22; PSD-95, p = 0.50). (B) Protein expression in PSD fractions

549   prepared from the frontal cortex and hippocampus. The protein loaded in lanes for

550   GluA1, GluA2, GluN2A, GluN2B, GluK2, and PSD-95 were 10 μg, and 20 μg for

551   GluD2. Except for GluD2, there was no significant difference between WT and

552   GluD1-KO mice in protein expression prepared from the PSD fractions of the frontal

553   cortex (GluA1, p = 0.50; GluA2, p = 0.99; GluN2A, p = 0.70; GluN2B, p = 0.43;

554   GluK2, p = 0.71; GluD2, p = 0.01; PSD-95, p = 0.68) or the hippocampus (GluA1, p =

555   0.27; GluA2, p = 0.76; GluN2A, p = 0.51; GluN2B, p = 0.49; GluK2, p = 0.50; GluD2,

556   p = 0.03; PSD-95, p = 0.89). All values presented are mean ± SEM from 3-4 experiments.

557   *p < 0.05, unpaired Student's t-test with Welch's correction. FC, the frontal cortex; HPC,

558   the hippocampus.

559

Discussion

561   To avoid the variability inherent in mixed genetic backgrounds and effects of closely

562   linked genes flanking the targeted locus, we generated GluD1-KO mice with a pure

563   C57BL/6N background and performed behavior analysis to assess GluD1 functions *in*

564   *vivo*. Our GluD1-KO mice showed hyperlocomotor activity, abnormal social behavior, a

565   deficit in contextual (but not cued) fear memory, and enhancement of depressive-like

566   behavior, that is partially consistent with the previous studies using *Grid1*[tm1Jnz] mice

567   [37,38].

568   We did not observe significant differences in either aggressive behavior in the

569   resident-intruder test, anxiety-related behavior evaluated by the open field test or the

570   light-dark transition test, or the elevated plus maze in our GluD1-KO mice compared to

571   WT mice, whereas robust aggression and lower anxiety-related behavior were observed

572   in $Grid1^{tm1Jnz}$ mice [37]. There are three conceivable possibilities that may explain the

573   different behavioral phenotypes between our GluD1-KO and the $Grid1^{tm1Jnz}$ mice. The

574   first possibility is the strain difference and flanking-genes effect. It is known that there are

575   mouse-strain difference in basal levels of both aggression [44,45] and anxiety [41–43,93].

576   Moreover, it remains a concern that flanking alleles of the target locus generated during

577   the backcrossing of ES cell-derived knockout mice to appropriate mice strains may

578   influence phenotype [53,57,58]. The $Grid1^{tm1Jnz}$ mouse was generated using the

579   129S6/SvEvTac ES cell line [40] followed by backcrossing to C57BL/6 strain 2–6 times

580   [37–39], so a phenotype difference may have arisen due to this. The second possibility is

581   deleterious effects of selection maker gene in the target locus on the neighboring genes

582   expression. The $Grid1^{tm1Jnz}$ mouse harbors the neomycin phosphotransferase cassette

583   that allowed the selection of homologous recombinants in the targeted allele [40].

584   However, such marker genes can interfere with the transcription and splicing of the

585   neighboring genes, thereby resulting in ambiguous genotype-phenotype relationships

586   [64–67]. The gene encoding microRNA (miRNA) *miR-346* that regulates the translation

587   of mRNAs via interaction with their 3' untranslated regions, is located in intron 2 of the

588   GluD1 gene [94]. In contrast, the neomycin phosphotransferase cassette in our

589   GluD1-KO mice deleted via the Cre/loxP system, so it is more appropriate for analyses

590   of GluD1 function. The third possibility is a gene-environment interaction where

591   differences in laboratory environments becomes an additional contributing factor that

592   modulates the behavioral outcome of genetically modified animal models in psychiatry

593   [95,96].

594   We found that there was no significant alteration of postsynaptic protein

595   expression, including AMPA-, kainite-, and NMDA-type glutamate receptor subunits,

596   and PSD-95, in the frontal cortex or the hippocampus of GluD1-KO mice, which is

597   inconsistent with the previous studies [37–39]. In the prefrontal cortex, a significantly

598   lower expression of GluA1 and GluA2 was observed in $Grid1^{tm1Jnz}$ mice [37]. In

599   addition, there was a significantly lower expression level of GluA1, GluA2, and GluK2,

600   and a significantly higher expression level of GluN2B and PSD-95 in the hippocampus of

601     $Grid1^{tm1Jnz}$ mice [38]. In that study, the authors used a quantification method for

602   synaptosome fraction in which the optical density of each protein of interest was

603   normalized to β-actin [37,38]. In this case, however, normalization of synaptosome

604   fraction by β-actin might be an inappropriate method for two reasons. Firstly, β-actin is a

605   cytoplasmic protein and synaptosomal preparation may increase the variability of the

606   amount of β-actin proteins in the synaptosome fractions. Secondly, Gupta and colleagues

607   suggested that morphological abnormality in the hippocampus and the medial prefrontal

608   cortex in $Grid1^{tm1Jnz}$ mice was probably due to an alteration of actin dynamics [39]. If

609   this was the case, then β-actin is not an appropriate protein for normalization. In contrast,

27

610   we investigated expression levels of synaptic proteins in synaptosome and PSD fractions

611   between WT and GluD1-KO mice using western blot without normalization by β-actin

612   (see Method). In addition, we confirmed that results of western blot for synaptosome and

613   PSD fractions without normalization were consistent with those on semi-quantitative

614   analysis using immunofluorescence [32,97–99].

615   In the fear conditioning test, GluD1-KO mice showed significantly lower freezing

616   times in contextual tests, but not in the cued tests. It is well known that the hippocampus

617   and amygdala are critical regions underlying contextual fear conditioning, whereas the

618   amygdala underlies cued conditioning [8]. The deficit of GluD1-KO mice in the

619   contextual test might suggest that GluD1 is more functionally important in the

620   hippocampus. Interestingly, forebrain-specific knockout mice of Cbln1, a partner

621   molecule of GluD1, showed a deficit in contextual and cued memory in the fear

622   conditioning test [100]. The GluD1-CBLN2-NRXN transsynaptic adhesion system

623   requires the formation and maintenance of synapses in the hippocampus *in vitro* and *ex*

624   *vivo* [1,2]. Moreover, Cbln1/2 double knockout mice have decreased synapse density in

625   the hippocampus of 6-month-olds but not 1- or 2-month-olds [3]. Of note, we observed

626   increased GluD2 expression in the PSD fraction of the hippocampus of GluD1-KO mice.

627   In contrast, increased GluD1 expression has been reported in the cerebellum of

628   GluD2-KO mice [9]. These results imply that compensatory regulation for GluD

629   subunits expression exists in brain regions, including the hippocampus. Further analysis

630   needs to clarify the specific role of the GluD-CBLN-NRXN transsynaptic adhesion

631   system in the hippocampus. In addition, there are reports that GluD1 also has unique

632   functions, such as (1) a regulator for group 5 mGluR-mediated AMPA-type glutamate

633   receptor trafficking [4], and (2) the ion channel activity via group 1 mGluR signaling

634   [5–7]. So, there are other possibilities that may explain how dysfunction of GluD1

635   affects hippocampal-dependent contextual fear memory. To determine details of the

636   molecular function of GluD1, the hippocampus is a suitable brain area for further

637   analyses.

638   Human GluD1 gene (*GRID1*) is a gene associated with susceptibility to

639   schizophrenia, autism spectrum disorder, and depression [23–28,94,101]. However,

640   how *GRID1* affects the pathophysiology of these conditions largely remains elusive.

641   Our GluD1-KO mice showed significantly lower sociability in the three-chambered

642   social interaction test, consistent with a previous report [37]. In contrast, our GluD1-KO

643   mice showed lower social novelty preference that is inconsistent with a previous report

644   [37]. Further analysis, such as novel object recognition, may clarify whether this

645   phenotype is derived from either impairment of memory function, sociability, or both.

646   Interestingly, lower *GRID1* mRNA expression is observed in the cerebral cortex of

647   patients with schizophrenia [94] and autism spectrum disorder [102]. Downregulation of

648   *GRID1* mRNA expression is also observed in iPS (induced pluripotent stem) cells

649   derived from Rett syndrome patients, which is a condition associated with autism

650   spectrum disorder [103]. In addition, downregulation of *Cbln1* mRNA was observed in

651   mice carrying a triple dose of Ube3a, a model mouse for autism spectrum disorder [104].

652   Deletion of *Cbln1* in the glutamatergic neurons of the ventral tegmental area led to

653   lower sociability by weakening excitatory synaptic transmission [104]. This behavioral

654   abnormality might support the hypothesis that GluD1-CBLN-NRXN-dependent synapse

655   formation and maintenance, in particular brain regions, is related to sociability.

656　　　　Our GluD1-KO mice showed enhanced depressive-like behavior assessed by the

657　　　forced-swim test. Pharmacological studies further revealed that imipramine and

658　　　fluoxetine, but not desipramine, significantly restored the enhanced depressive-like

659　　　behavior in GluD1-KO mice. Because imipramine and fluoxetine are more effective in

660　　　inhibiting serotonin transporters than desipramine [91,92], increased serotonin

661　　　concentration in the brain regions related to depressive-like behavior may account for

662　　　the abnormal behavior of GluD1-KO mice; in other words, the serotonin signaling

663　　　pathway might be altered in GluD1-KO mice. Candidate regions, in which GluD1 is

664　　　expressed, related to depression are the lateral habenula and dorsal raphe nucleus

665　　　[32,33,100]. Increased neuronal activity in the lateral habenula is observed in patients

666　　　with depression and in animal models of depression [105,106] and lesions of the lateral

667　　　habenula alters extracellular serotonin concentration in the dorsal raphe nucleus when

668　　　receiving uncontrollable stress [107]. Furthermore, GluD1 mRNA is downregulated in

669　　　the frontal cortex of anhedonic rats as an animal model of depression [108], and this

670　　　phenotype is completely reversed by intraperitoneal injection of the antipsychotic

671　　　quetiapine [109]. Further analysis is required to identify regions involved in the

672　　　enhanced depressive-like behavior mediated by the serotonergic system in GluD1-KO

673　　　mice. As to the effect of antidepressants in the forced-swim test, selective serotonin

674　　　reuptake inhibitors (SSRIs) tend to lead to more swimming behavior, whereas serotonin

675　　　and norepinephrine reuptake inhibitors (SNRIs) tend to lead to more climbing behavior

676　　　[110,111]. Thus, evaluating climbing and swimming behavior with more specific SSRIs

677　　　(e.g. citalopram or escitalopram) [91,112] and SNRIs (e.g. reboxetine or atomoxetine)

678　　　[113] will allow us to more precisely discriminate the pathway underlying enhanced

679　　　depressive-like behavior in GluD1-KO mice.

680   Behavioral analyses under a pure C57BL/6N genetic background suggest that

681   GluD1 plays critical roles in contextual fear memory, sociability, and depressive-like

682   behavior. We originally developed the *Grid1*$^{+/flox}$ mouse in which exon 4 of *Grid1* gene

683   was flanked by loxP sequences [68]. *Grid1*$^{flox/flox}$ mice under a C57BL/6N genetic

684   background allow us to delete the *Grid1* gene in a brain region-specific manner using

685   region-specific Cre mice or Cre-expressing virus injections. This brain region-specific

686   GluD1-KO mouse could be a useful tool to clarify the neuronal circuits and molecular

687   mechanisms involved in contextual fear memory, sociability, and depressive-like

688   behavior.

689

Acknowledgments

690

695

Author contributions

696

697   1.   Conceptualization: CN, MA, KS.

698   2.   Formal analysis: CN, TT.

699   3.   Funding acquisition: TT, KS.

700   4.   Investigation: CN.

701   5.   Methodology: CN, MK, MA, KS.

702   6.   Project administration: MA, KS.

703   7.   Resources: EN, RN, MW.

704   8.   Validation: CN, KT, TT.

705   9.   Visualization: CN, TT.

706   10.   Writing – original draft: CN, TT.

707   11.   Writing – review & editing: CN, MK, KT, MW, MA, TT, KS.

708   All authors discussed the manuscript.

709

Conflict of interest

711   The authors declare no competing financial interests.

712

Data Availability Statement

714   All the raw data of behavioral tests (doi: 10.6084/m9.figshare.10052663) and western

715   blot images (doi: 10.6084/m9.figshare.10053092) in this study are disclosed in the

716   figshare.

717

Funding

725

726

727

728

729

References

731   1.   Yamazaki M, Araki K, Shibata A, Mishina M. Molecular cloning of a cDNA

732   encoding a novel member of the mouse glutamate receptor channel family.

733   Biochem Biophys Res Commun. 1992;183: 886–892.

734   doi:10.1016/0006-291X(92)90566-4

735   2.   Araki K, Meguro H, Kushiya E, Takayama C, Inoue Y, Mishina M. Selective

736   expression of the glutamate receptor channel delta 2 subunit in cerebellar Purkinje

737   cells. Biochem Biophys Res Commun. 1993;197: 1267–76.

738   doi:10.1006/bbrc.1993.2614

739   3.   Lomeli H, Sprengel R, Laurie DJ, Köhr G, Herb A, Seeburg PH, et al. The rat

740   delta-1 and delta-2 subunits extend the excitatory amino acid receptor family.

741   FEBS Lett. 1993;315: 318–322. doi:10.1016/0014-5793(93)81186-4

742   4.   Hirai H, Miyazaki T, Kakegawa W, Matsuda S, Mishina M, Watanabe M, et al.

743   Rescue of abnormal phenotypes of the delta2 glutamate receptor-null mice by

744   mutant delta2 transgenes. EMBO Rep. 2005;6: 90–5.

745   doi:10.1038/sj.embor.7400312

746   5.   Kakegawa W, Kohda K, Yuzaki M. The delta2 "ionotropic" glutamate receptor

747   functions as a non-ionotropic receptor to control cerebellar synaptic plasticity. J

748   Physiol. 2007;584: 89–96. doi:10.1113/jphysiol.2007.141291

749   6.   Kakegawa W, Miyazaki T, Hirai H, Motohashi J, Mishina M, Watanabe M, et al.

750   Ca2+ permeability of the channel pore is not essential for the delta2 glutamate

751   receptor to regulate synaptic plasticity and motor coordination. J Physiol.

752   2007;579: 729–35. doi:10.1113/jphysiol.2006.127100

753   7.   Matsuda K, Miura E, Miyazaki T, Kakegawa W, Emi K, Narumi S, et al. Cbln1 is

754   a ligand for an orphan glutamate receptor delta2, a bidirectional synapse organizer.

755   Science. 2010;328: 363–8. doi:10.1126/science.1185152

756   8.   Uemura T, Lee S-J, Yasumura M, Takeuchi T, Yoshida T, Ra M, et al.

757   Trans-synaptic interaction of GluRdelta2 and Neurexin through Cbln1 mediates

758   synapse formation in the cerebellum. Cell. 2010;141: 1068–79.

759   doi:10.1016/j.cell.2010.04.035

760   9.   Tao W, Díaz-Alonso J, Sheng N, Nicoll RA. Postsynaptic δ1 glutamate receptor

761   assembles and maintains hippocampal synapses via Cbln2 and neurexin. Proc Natl

762   Acad Sci U S A. 2018;115: E5373–E5381. doi:10.1073/pnas.1802737115

763   10.   Ady V, Perroy J, Tricoire L, Piochon C, Dadak S, Chen X, et al. Type 1

764   metabotropic glutamate receptors (mGlu1) trigger the gating of GluD2 delta

765   glutamate receptors. EMBO Rep. 2014;15: 103–9. doi:10.1002/embr.201337371

766   11.   Dadak S, Bouquier N, Goyet E, Fagni L, Levenes C, Perroy J. mGlu1 receptor

767   canonical signaling pathway contributes to the opening of the orphan GluD2

768   receptor. Neuropharmacology. 2017;115: 92–99.

769   doi:10.1016/J.NEUROPHARM.2016.06.001

770   12.   Benamer N, Marti F, Lujan R, Hepp R, Aubier TG, Dupin AAM, et al. GluD1,

771   linked to schizophrenia, controls the burst firing of dopamine neurons. Mol

772   Psychiatry. 2018;23: 691–700. doi:10.1038/mp.2017.137

773   13.   Takayama C, Nakagawa S, Watanabe M, Mishina M, Inoue Y. Light- and

774   electron-microscopic localization of the glutamate receptor channel 62 subunit in

775   the mouse Purkinje cell. Neurosci Lett. 1995;188: 89–92.

776   doi:10.1016/0304-3940(95)11403-J

777   14.   Landsend AS, Amiry-Moghaddam M, Matsubara A, Bergersen L, Usami S,

778   Wenthold RJ, et al. Differential Localization of delta Glutamate Receptors in the

779   Rat Cerebellum: Coexpression with AMPA Receptors in Parallel Fiber-Spine

780   Synapses and Absence from Climbing Fiber-Spine Synapses. J Neurosci. 1997;17:

781   834–842. Available: http://www.jneurosci.org/content/17/2/834.long

782 15. Kashiwabuchi N, Ikeda K, Araki K, Hirano T, Shibuki K, Takayama C, et al.

783   Impairment of motor coordination, Purkinje cell synapse formation, and cerebellar

784   long-term depression in GluRδ2 mutant mice. Cell. 1995;81: 245–252.

785   doi:10.1016/0092-8674(95)90334-8

786 16. Takeuchi T, Miyazaki T, Watanabe M, Mori H, Sakimura K, Mishina M. Control

787   of synaptic connection by glutamate receptor delta2 in the adult cerebellum. J

788   Neurosci. 2005;25: 2146–56. doi:10.1523/JNEUROSCI.4740-04.2005

789 17. Hirano T, Kasono K, Araki K, Shinozuka K, Mishina M. Involvement of the

790   glutamate receptor δ2 subunit in the long-term depression of glutamate

791   responsiveness in cultured rat Purkinje cells. Neurosci Lett. 1994;182: 172–176.

792   doi:10.1016/0304-3940(94)90790-0

793 18. Kishimoto Y, Kawahara S, Suzuki M, Mori H, Mishina M, Kirino Y. Classical

794   eyeblink conditioning in glutamate receptor subunit δ2 mutant mice is impaired in

795   the delay paradigm but not in the trace paradigm. Eur J Neurosci. 2001;13:

796   1249–1253. doi:10.1046/j.0953-816x.2001.01488.x

797   19.   Katoh A, Yoshida T, Himeshima Y, Mishina M, Hirano T. Defective control and

798   adaptation of reflex eye movements in mutant mice deficient in either the

799   glutamate receptor δ2 subunit or Purkinje cells. Eur J Neurosci. 2005;21:

800   1315–1326. doi:10.1111/j.1460-9568.2005.03946.x

801   20.   Kakegawa W, Miyazaki T, Emi K, Matsuda K, Kohda K, Motohashi J, et al.

802   Differential regulation of synaptic plasticity and cerebellar motor learning by the

803   C-terminal PDZ-binding motif of GluRdelta2. J Neurosci. 2008;28: 1460–8.

804   doi:10.1523/JNEUROSCI.2553-07.2008

805   21.   Takeuchi T, Ohtsuki G, Yoshida T, Fukaya M, Wainai T, Yamashita M, et al.

806   Enhancement of Both Long-Term Depression Induction and Optokinetic Response

807   Adaptation in Mice Lacking Delphilin. Grant SGN, editor. PLoS One. 2008;3:

808   e2297. doi:10.1371/journal.pone.0002297

809   22.   Kohda K, Kakegawa W, Matsuda S, Yamamoto T, Hirano H, Yuzaki M. The δ2

810   glutamate receptor gates long-term depression by coordinating interactions

811   between two AMPA receptor phosphorylation sites. Proc Natl Acad Sci U S A.

812   2013; 1218380110-. doi:10.1073/pnas.1218380110

813   23.   Fallin MD, Lasseter VK, Avramopoulos D, Nicodemus KK, Wolyniec PS,

814   McGrath JA, et al. Bipolar I Disorder and Schizophrenia: A

815   440–Single-Nucleotide Polymorphism Screen of 64 Candidate Genes among

816   Ashkenazi Jewish Case-Parent Trios. Am J Hum Genet. 2005;77: 918–936.

817   doi:10.1086/497703

818 24. Guo S-Z, Huang K, Shi Y-Y, Tang W, Zhou J, Feng G-Y, et al. A case-control

819   association study between the GRID1 gene and schizophrenia in the Chinese

820   Northern Han population. Schizophr Res. 2007;93: 385–90.

821   doi:10.1016/j.schres.2007.03.007

822 25. Treutlein J, Mühleisen TW, Frank J, Mattheisen M, Herms S, Ludwig KU, et al.

823   Dissection of phenotype reveals possible association between schizophrenia and

824   Glutamate Receptor Delta 1 (GRID1) gene promoter. Schizophr Res. 2009;111:

825   123–130. doi:10.1016/j.schres.2009.03.011

826 26. Chen X, Lee G, Maher BS, Fanous AH, Chen J, Zhao Z, et al. GWA study data

827   mining and independent replication identify cardiomyopathy-associated 5

828   (CMYA5) as a risk gene for schizophrenia. Mol Psychiatry. 2011;16: 1117–29.

829   doi:10.1038/mp.2010.96

830 27. Muglia P, Tozzi F, Galwey NW, Francks C, Upmanyu R, Kong XQ, et al.

831   Genome-wide association study of recurrent major depressive disorder in two

832   European case–control cohorts. Mol Psychiatry. 2010;15: 589–601.

833   doi:10.1038/mp.2008.131

834   28.   Glessner JT, Wang K, Cai G, Korvatska O, Kim CE, Wood S, et al. Autism

835   genome-wide copy number variation reveals ubiquitin and neuronal genes. Nature.

836   2009;459: 569–573. doi:10.1038/nature07953

837   29.   Smith M, Spence MA, Flodman P. Nuclear and Mitochondrial Genome Defects in

838   Autisms. Ann N Y Acad Sci. 2009;1151: 102–132.

839   doi:10.1111/j.1749-6632.2008.03571.x

840   30.   Griswold AJ, Ma D, Cukier HN, Nations LD, Schmidt MA, Chung R-H, et al.

841   Evaluation of copy number variations reveals novel candidate genes in autism

842   spectrum disorder-associated pathways. Hum Mol Genet. 2012;21: 3513–23.

843   doi:10.1093/hmg/dds164

844   31.   Nord AS, Roeb W, Dickel DE, Walsh T, Kusenda M, O'Connor KL, et al.

845   Reduced transcript expression of genes affected by inherited and de novo CNVs in

846   autism. Eur J Hum Genet. 2011;19: 727–31. doi:10.1038/ejhg.2011.24

847   32.   Konno K, Matsuda K, Nakamoto C, Uchigashima M, Miyazaki T, Yamasaki M, et

848   al. Enriched expression of GluD1 in higher brain regions and its involvement in

849   parallel fiber-interneuron synapse formation in the cerebellum. J Neurosci.

850   2014;34: 7412–24. doi:10.1523/JNEUROSCI.0628-14.2014

851 33. Hepp R, Hay YA, Aguado C, Lujan R, Dauphinot L, Potier MC, et al. Glutamate

852   receptors of the delta family are widely expressed in the adult brain. Brain Struct

853   Funct. 2015;220: 2797–2815. doi:10.1007/s00429-014-0827-4

854 34. Ryu K, Yokoyama M, Yamashita M, Hirano T. Induction of excitatory and

855   inhibitory presynaptic differentiation by GluD1. Biochem Biophys Res Commun.

856   2012;417: 157–61. doi:10.1016/j.bbrc.2011.11.075

857 35. Yasumura M, Yoshida T, Lee S, Uemura T, Joo J, Mishina M. Glutamate receptor

858   δ1 induces preferentially inhibitory presynaptic differentiation of cortical neurons

859   by interacting with neurexins through cerebellin precursor protein subtypes. J

860   Neurochem. 2012;121: 705–716. doi:10.1111/J.1471-4159.2011.07631.X

861 36. Suryavanshi PS, Gupta SC, Yadav R, Kesherwani V, Liu J, Dravid SM. Glutamate

862   Delta-1 Receptor Regulates Metabotropic Glutamate Receptor 5 Signaling in the

863   Hippocampus. Mol Pharmacol. 2016;90: 96–105. doi:10.1124/mol.116.104786

864 37. Yadav R, Gupta SC, Hillman BG, Bhatt JM, Stairs DJ, Dravid SM. Deletion of

865   glutamate delta-1 receptor in mouse leads to aberrant emotional and social

866   behaviors. Christie B, editor. PLoS One. 2012;7: e32969.

867   doi:10.1371/journal.pone.0032969

868   38.   Yadav R, Hillman BG, Gupta SC, Suryavanshi P, Bhatt JM, Pavuluri R, et al.

869   Deletion of Glutamate Delta-1 Receptor in Mouse Leads to Enhanced Working

870   Memory and Deficit in Fear Conditioning. Christie B, editor. PLoS One. 2013;8:

871   e60785. doi:10.1371/journal.pone.0060785

872   39.   Gupta SC, Yadav R, Pavuluri R, Morley BJ, Stairs DJ, Dravid SM. Essential role

873   of GluD1 in dendritic spine development and GluN2B to GluN2A NMDAR

874   subunit switch in the cortex and hippocampus reveals ability of GluN2B inhibition

875   in correcting hyperconnectivity. Neuropharmacology. 2015;93: 274–284.

876   doi:10.1016/j.neuropharm.2015.02.013

877   40.   Gao J, Maison SF, Wu X, Hirose K, Jones SM, Bayazitov I, et al. Orphan

878   glutamate receptor delta1 subunit required for high-frequency hearing. Mol Cell

879   Biol. 2007;27: 4500–12. doi:10.1128/MCB.02051-06

880   41.   Crawley JN, Belknap JK, Collins A, Crabbe JC, Frankel W, Henderson N, et al.

881   Behavioral phenotypes of inbred mouse strains: implications and

882   recommendations for molecular studies. Psychopharmacology (Berl). 1997;132:

883   107–124. doi:10.1007/s002130050327

884   42.   Holmes A, Li Q, Murphy DL, Gold E, Crawley JN. Abnormal anxiety-related

885   behavior in serotonin transporter null mutant mice: the influence of genetic

886   background. Genes, Brain Behav. 2003;2: 365–380.

887   doi:10.1046/j.1601-1848.2003.00050.x

888   43.   Holmes A. Targeted gene mutation approaches to the study of anxiety-like

889   behavior in mice [Internet]. Pergamon; May 1, 2001 pp. 261–273.

890   doi:10.1016/S0149-7634(01)00012-4

891   44.   Kessler S, Elliott GR, Orenberg EK, Barchas JD. A genetic analysis of aggressive

892   behavior in two strains of mice. Behav Genet. 1977;7: 313–21. Available:

893   http://www.ncbi.nlm.nih.gov/pubmed/562156

894   45.   Mineur YS, Prasol DJ, Belzung C, Crusio WE. Agonistic Behavior and

895   Unpredictable Chronic Mild Stress in Mice. Behav Genet. 2003;33: 513–519.

896   doi:10.1023/A:1025770616068

897   46.   Paylor R, Crawley JN. Inbred strain differences in prepulse inhibition of the mouse

898   startle response. Psychopharmacology (Berl). 1997;132: 169–80. Available:

899   http://www.ncbi.nlm.nih.gov/pubmed/9266614

900   47.   Moy SS, Nadler JJ, Young NB, Perez A, Holloway LP, Barbaro RP, et al. Mouse

901   behavioral tasks relevant to autism: Phenotypes of 10 inbred strains. Behav Brain

902   Res. 2007;176: 4–20. doi:10.1016/J.BBR.2006.07.030

903   48.   Moy SS, Nadler JJ, Perez A, Barbaro RP, Johns JM, Magnuson TR, et al.

904   Sociability and preference for social novelty in five inbred strains: an approach to

905   assess autistic-like behavior in mice. Genes, Brain Behav. 2004;3: 287–302.

906   doi:10.1111/j.1601-1848.2004.00076.x

907   49.   Mogil JS, Wilson SG, Bon K, Eun Lee S, Chung K, Raber P, et al. Heritability of

908   nociception I: Responses of 11 inbred mouse strains on 12 measures of nociception.

909   Pain. 1999;80: 67–82. doi:10.1016/S0304-3959(98)00197-3

910   50.   Mineur YS, Belzung C, Crusio WE. Effects of unpredictable chronic mild stress on

911   anxiety and depression-like behavior in mice. Behav Brain Res. 2006;175: 43–50.

912   doi:10.1016/J.BBR.2006.07.029

913   51.   Lucki I, Dalvi A, Mayorga A. Sensitivity to the effects of pharmacologically

914   selective antidepressants in different strains of mice. Psychopharmacology (Berl).

915   2001;155: 315–322. doi:10.1007/s002130100694

916   52.   Holmes A, Yang RJ, Murphy DL, Crawley JN. Evaluation of

917   antidepressant-related behavioral responses in mice lacking the serotonin

44

918   transporter. Neuropsychopharmacology. 2002;27: 914–23.

919   doi:10.1016/S0893-133X(02)00374-3

920   53.   Gerlai R. Gene-targeting studies of mammalian behavior: is it the mutation or the

921   background genotype? Trends Neurosci. 1996;19: 177–181.

922   doi:10.1016/S0166-2236(96)20020-7

923   54.   Wolfer DP, Müller U, Stagliar M, Lipp H-P. Assessing the effects of the 129/Sv

924   genetic background on swimming navigation learning in transgenic mutants: a

925   study using mice with a modified β-amyloid precursor protein gene. Brain Res.

926   1997;771: 1–13. doi:10.1016/S0006-8993(97)00673-2

927   55.   Owen E., Logue S., Rasmussen D., J. M. Wehner. Assessment of learning by the

928   Morris water task and fear conditioning in inbred mouse strains and F1 hybrids:

929   implications of genetic background for single gene mutations and quantitative trait

930   loci analyses. Neuroscience. 1997;80: 1087–1099.

931   doi:10.1016/S0306-4522(97)00165-6

932   56.   Balogh SA, Wehner JM. Inbred mouse strain differences in the establishment of

933   long-term fear memory. Behav Brain Res. 2003;140: 97–106.

934   doi:10.1016/S0166-4328(02)00279-6

935   57.   Crusio WE. Flanking gene and genetic background problems in genetically

936   manipulated mice. Biol Psychiatry. 2004;56: 381–385.

937   doi:10.1016/J.BIOPSYCH.2003.12.026

938   58.   Phillips TJ, Hen R, Crabbe JC. Complications associated with genetic background

939   effects in research using knockout mice. Psychopharmacology (Berl). 1999;147:

940   5–7. doi:10.1007/s002130051128

941   59.   Koike H, Arguello PA, Kvajo M, Karayiorgou M, Gogos JA. Disc1 is mutated in

942   the 129S6/SvEv strain and modulates working memory in mice. Proc Natl Acad

943   Sci U S A. 2006;103: 3693–7. doi:10.1073/pnas.0511189103

944   60.   Clapcote SJ, Roder JC. Deletion polymorphism of Disc1 is common to all 129

945   mouse substrains: implications for gene-targeting studies of brain function.

946   Genetics. 2006;173: 2407–10. doi:10.1534/genetics.106.060749

947   61.   Kuroda K, Yamada S, Tanaka M, Iizuka M, Yano H, Mori D, et al. Behavioral

948   alterations associated with targeted disruption of exons 2 and 3 of the Disc1 gene

949   in the mouse. Hum Mol Genet. 2011;20: 4666–4683. doi:10.1093/hmg/ddr400

950   62.   Blackwood DHR, Fordyce A, Walker MT, St. Clair DM, Porteous DJ, Muir WJ.

951   Schizophrenia and Affective Disorders—Cosegregation with a Translocation at

952   Chromosome 1q42 That Directly Disrupts Brain-Expressed Genes: Clinical and

953   P300 Findings in a Family. Am J Hum Genet. 2001;69: 428–433.

954   doi:10.1086/321969

955 63. Kilpinen H, Ylisaukko-oja T, Hennah W, Palo OM, Varilo T, Vanhala R, et al.

956   Association of DISC1 with autism and Asperger syndrome. Mol Psychiatry.

957   2008;13: 187–196. doi:10.1038/sj.mp.4002031

958 64. Fiering S, Epner E, Robinson K, Zhuang Y, Telling A, Hu M, et al. Targeted

959   deletion of 5'HS2 of the murine beta-globin LCR reveals that it is not essential for

960   proper regulation of the beta-globin locus. Genes Dev. 1995;9: 2203–13.

961   doi:10.1101/gad.9.18.2203

962 65. Mishina M, Sakimura K. Conditional gene targeting on the pure C57BL/6 genetic

963   background. Neurosci Res. 2007;58: 105–112.

964   doi:10.1016/J.NEURES.2007.01.004

965 66. Olson EN, Arnold HH, Rigby PWJ, Wold BJ. Know your neighbors: Three

966   phenotypes in null mutants of the myogenic bHLH gene MRF4 [Internet]. Cell.

967   Elsevier; 1996. pp. 1–4. doi:10.1016/S0092-8674(00)81073-9

968 67. Pham CT, MacIvor DM, Hug BA, Heusel JW, Ley TJ. Long-range disruption of

969   gene expression by a selectable marker cassette. Proc Natl Acad Sci U S A.

970   1996;93: 13090–5. doi:10.1073/PNAS.93.23.13090

971   68.   Nakamoto C, Konno K, Miyazaki T, Nakatsukasa E, Natsume R, Abe M, et al.

972   Expression mapping, quantification, and complex formation of GluD1 and GluD2

973   glutamate receptors in adult mouse brain. J Comp Neurol. 2019;In press.

974   doi:10.1002/cne.24792

975   69.   Nakamura K, Manabe T, Watanabe M, Mamiya T, Ichikawa R, Kiyama Y, et al.

976   Enhancement of hippocampal LTP, reference memory and sensorimotor gating in

977   mutant mice lacking a telencephalon-specific cell adhesion molecule. Eur J

978   Neurosci. 2001;13: 179–189. doi:10.1046/j.0953-816X.2000.01366.x

979   70.   Katano T, Takao K, Abe M, Yamazaki M, Watanabe M, Miyakawa T, et al.

980   Distribution of Caskin1 protein and phenotypic characterization of its knockout

981   mice using a comprehensive behavioral test battery. Mol Brain. 2018;11: 63.

982   doi:10.1186/s13041-018-0407-2

983   71.   Kato T, Kasai A, Mizuno M, Fengyi L, Shintani N, Maeda S, et al. Phenotypic

984   characterization of transgenic mice overexpressing neuregulin-1. PLoS One.

985   2010;5: e14185. doi:10.1371/journal.pone.0014185

986   72.   Porsolt RD, Le Pichon M, Jalfre M. Depression: a new animal model sensitive to

987   antidepressant treatments. Nature. 1977;266: 730–732. doi:10.1038/266730a0

988   73.   Redrobe JP, MacSweeney CP, Bourin M. The role of 5-HT1A and 5-HT1B

989   receptors in antidepressant drug actions in the mouse forced swimming test. Eur J

990   Pharmacol. 1996;318: 213–220. doi:10.1016/S0014-2999(96)00772-8

991   74.   Vaugeois J-M, Passera G, Zuccaro F, Costentin J. Individual differences in

992   response to imipramine in the mouse tail suspension test. Psychopharmacology

993   (Berl). 1997;134: 387–391. doi:10.1007/s002130050475

994   75.   Harkin AJ, Bruce KH, Craft B, Paul IA. Nitric oxide synthase inhibitors have

995   antidepressant-like properties in mice: 1. Acute treatments are active in the forced

996   swim test. Eur J Pharmacol. 1999;372: 207–213.

997   doi:10.1016/S0014-2999(99)00191-0

998   76.   Wong EHF, Sonders MS, Amara SG, Tinholt PM, Piercey MFP, Hoffmann WP, et

999   al. Reboxetine: a pharmacologically potent, selective, and specific norepinephrine

1000   reuptake inhibitor. Biol Psychiatry. 2000;47: 818–829.

1001   doi:10.1016/S0006-3223(99)00291-7

1002   77.   Zhang H, Li Z, Zhou Z, Yang H, Zhong Z, Lou C. Antidepressant-like effects of

1003   ginsenosides: A comparison of ginsenoside Rb3 and its four deglycosylated

1004   derivatives, Rg3, Rh2, compound K, and 20(S)-protopanaxadiol in mice models of

1005   despair. Pharmacol Biochem Behav. 2016;140: 17–26.

1006   doi:10.1016/J.PBB.2015.10.018

1007   78.   Liu X, Gershenfeld HK. Genetic differences in the tail-suspension test and its

1008   relationship to imipramine response among 11 inbred strains of mice. Biol

1009   Psychiatry. 2001;49: 575–581. doi:10.1016/S0006-3223(00)01028-3

1010   79.   Carlin RK. Isolation and characterization of postsynaptic densities from various

1011   brain regions: enrichment of different types of postsynaptic densities. J Cell Biol.

1012   1980;86: 831–845. doi:10.1083/jcb.86.3.831

1013   80.   Yamazaki M, Fukaya M, Hashimoto K, Yamasaki M, Tsujita M, Itakura M, et al.

1014   TARPs gamma-2 and gamma-7 are essential for AMPA receptor expression in the

1015   cerebellum. Eur J Neurosci. 2010;31: 2204–20.

1016   doi:10.1111/j.1460-9568.2010.07254.x

1017   81.   Watanabe M, Fukaya M, Sakimura K, Manabe T, Mishina M, Inoue Y. Selective

1018   scarcity of NMDA receptor channel subunits in the stratum lucidum (mossy

1019   fibre□recipient layer) of the mouse hippocampal CA3 subfield. Eur J Neurosci.

1020   1998;10: 478–487. doi:10.1046/j.1460-9568.1998.00063.x

1021   82.   Watanabe-Iida I, Konno K, Akashi K, Abe M, Natsume R, Watanabe M, et al.

1022   Determination of kainate receptor subunit ratios in mouse brain using novel

1023   chimeric protein standards. J Neurochem. 2016;136: 295–305.

1024   doi:10.1111/jnc.13384

1025   83.   Fukaya M, Watanabe M. Improved immunohistochemical detection of

1026   postsynaptically located PSD-95/SAP90 protein family by protease section

1027   pretreatment: A study in the adult mouse brain. J Comp Neurol. 2000;426:

1028   572–586. doi:10.1002/1096-9861(20001030)426:4<572::AID-CNE6>3.0.CO;2-9

1029   84.   Valle FP. Effects of Strain, Sex, and Illumination on Open-Field Behavior of Rats.

1030   Am J Psychol. 1970;83: 103. doi:10.2307/1420860

1031   85.   Griebel G, Moreau J-L, Jenck F, Martin JR, Misslin R. Some critical determinants

1032   of the behaviour of rats in the elevated plus-maze. Behav Processes. 1993;29:

1033   37–47. doi:10.1016/0376-6357(93)90026-N

1034   86.   Crawley JN. Behavioral Phenotyping Strategies for Mutant Mice. Neuron.

1035   2008;57: 809–818. doi:10.1016/J.NEURON.2008.03.001

1036   87.   Braff D, Stone C, Callaway E, Geyer M, Glick I, Bali L. Prestimulus Effects on

1037   Human Startle Reflex in Normals and Schizophrenics. Psychophysiology.

1038   1978;15: 339–343. doi:10.1111/j.1469-8986.1978.tb01390.x

1039 88. Grillon C, Ameli R, Charney DS, Krystal J, Braff D. Startle gating deficits occur

1040   across prepulse intensities in schizophrenic patients. Biol Psychiatry. 1992;32:

1041   939–43. Available: http://www.ncbi.nlm.nih.gov/pubmed/1467378

1042 89. Braff DL, Geyer MA. Sensorimotor Gating and Schizophrenia. Arch Gen

1043   Psychiatry. 1990;47: 181. doi:10.1001/archpsyc.1990.01810140081011

1044 90. Swerdlow NR, Braff DL, Taaid N, Geyer MA. Assessing the validity of an animal

1045   model of deficient sensorimotor gating in schizophrenic patients. Arch Gen

1046   Psychiatry. 1994;51: 139–54. Available:

1047   http://www.ncbi.nlm.nih.gov/pubmed/8297213

1048 91. Tatsumi M, Groshan K, Blakely RD, Richelson E. Pharmacological profile of

1049   antidepressants and related compounds at human monoamine transporters. Eur J

1050   Pharmacol. 1997;340: 249–258. doi:10.1016/S0014-2999(97)01393-9

1051 92. Owens MJ, Morgan WN, Plott SJ, Nemeroff CB. Neurotransmitter receptor and

1052   transporter binding profile of antidepressants and their metabolites. J Pharmacol

1053   Exp Ther. 1997;283: 1305–22. Available:

1054   http://www.ncbi.nlm.nih.gov/pubmed/9400006

1055 93. Crawley JN. Unusual behavioral phenotypes of inbred mouse strains. Trends

1056   Neurosci. 1996;19: 181–182. doi:10.1016/S0166-2236(96)20021-9

1057   94.   Zhu Y, Kalbfleisch T, Brennan MD, Li Y. A MicroRNA gene is hosted in an intron

1058   of a schizophrenia-susceptibility gene. Schizophrenia Research. 2009.

1059   doi:10.1016/j.schres.2009.01.022

1060   95.   Crabbe JC, Wahlsten D, Dudek BC. Genetics of Mouse Behavior: Interactions

1061   with Laboratory Environment. Science (80-). 1999;284. Available:

1062   http://science.sciencemag.org/content/284/5420/1670.full

1063   96.   Razafsha M, Behforuzi H, Harati H, Wafai RA, Khaku A, Mondello S, et al. An

1064   updated overview of animal models in neuropsychiatry. Neuroscience. 2013;240:

1065   204–218. doi:10.1016/J.NEUROSCIENCE.2013.02.045

1066   97.   Abe M, Fukaya M, Yagi T, Mishina M, Watanabe M, Sakimura K. NMDA

1067   receptor GluRepsilon/NR2 subunits are essential for postsynaptic localization and

1068   protein stability of GluRzeta1/NR1 subunit. J Neurosci. 2004;24: 7292–304.

1069   doi:10.1523/JNEUROSCI.1261-04.2004

1070   98.   Akashi K, Kakizaki T, Kamiya H, Fukaya M, Yamasaki M, Abe M, et al. NMDA

1071   receptor GluN2B (GluR epsilon 2/NR2B) subunit is crucial for channel function,

1072   postsynaptic macromolecular organization, and actin cytoskeleton at hippocampal

1073   CA3 synapses. J Neurosci. 2009;29: 10869–82.

1074   doi:10.1523/JNEUROSCI.5531-08.2009

1075   99.   Kawakami R, Shinohara Y, Kato Y, Sugiyama H, Shigemoto R, Ito I.

1076   Asymmetrical allocation of NMDA receptor epsilon2 subunits in hippocampal

1077   circuitry. Science. 2003;300: 990–4. doi:10.1126/science.1082609

1078   100. Otsuka S, Konno K, Abe M, Motohashi J, Kohda K, Sakimura K, et al. Roles of

1079   Cbln1 in Non-Motor Functions of Mice. J Neurosci. 2016;36: 11801–11816.

1080   doi:10.1523/JNEUROSCI.0322-16.2016

1081   101. Edwards AC, Aliev F, Bierut LJ, Bucholz KK, Edenberg H, Hesselbrock V, et al.

1082   Genome-wide association study of comorbid depressive syndrome and alcohol

1083   dependence. Psychiatr Genet. 2012;22: 31–41.

1084   doi:10.1097/YPG.0b013e32834acd07

1085   102. Garbett K, Ebert PJ, Mitchell A, Lintas C, Manzi B, Mirnics K, et al. Immune

1086   transcriptome alterations in the temporal cortex of subjects with autism. Neurobiol

1087   Dis. 2008;30: 303–311. Available:

1088   https://www.sciencedirect.com/science/article/pii/S0969996108000247?via%3Di

1089   hub

1090   103. Livide G, Patriarchi T, Amenduni M, Amabile S, Yasui D, Calcagno E, et al.

1091   GluD1 is a common altered player in neuronal differentiation from both

1092   MECP2-mutated and CDKL5-mutated iPS cells. Eur J Hum Genet. 2015;23:

1093   195–201. doi:10.1038/ejhg.2014.81

1094   104. Krishnan V, Stoppel DC, Nong Y, Johnson MA, Nadler MJS, Ozkaynak E, et al.

1095   Autism gene Ube3a and seizures impair sociability by repressing VTA Cbln1.

1096   Nature. 2017;543: 507–512. doi:10.1038/nature21678

1097   105. Li B, Piriz J, Mirrione M, Chung C, Proulx CD, Schulz D, et al. Synaptic

1098   potentiation onto habenula neurons in the learned helplessness model of

1099   depression. Nature. 2011;470: 535–539. doi:10.1038/nature09742

1100   106. Li K, Zhou T, Liao L, Yang Z, Wong C, Henn F, et al. CaMKII in Lateral

1101   Habenula Mediates Core Symptoms of Depression. Science (80-). 2013;341:

1102   1016–1020. doi:10.1126/science.1240729

1103   107. Amat J, Sparks PD, Matus-Amat P, Griggs J, Watkins LR, Maier SF. The role of

1104   the habenular complex in the elevation of dorsal raphe nucleus serotonin and the

1105   changes in the behavioral responses produced by uncontrollable stress. Brain Res.

1106   2001;917: 118–126. doi:10.1016/S0006-8993(01)02934-1

1107   108. Orsetti M, Di Brisco F, Canonico PL, Genazzani AA, Ghi P. Gene regulation in the

1108   frontal cortex of rats exposed to the chronic mild stress paradigm, an animal model

1109   of human depression. Eur J Neurosci. 2008;27: 2156–2164.

1110   doi:10.1111/j.1460-9568.2008.06155.x

1111   109. Orsetti M, Di Brisco F, Rinaldi M, Dallorto D, Ghi P. Some molecular effectors of

1112   antidepressant action of quetiapine revealed by DNA microarray in the frontal

1113   cortex of anhedonic rats. Pharmacogenet Genomics. 2009;19: 600–12.

1114   doi:10.1097/FPC.0b013e32832ee573

1115   110. Rénéric J-P, Lucki I. Antidepressant behavioral effects by dual inhibition of

1116   monoamine reuptake in the rat forced swimming test. Psychopharmacology (Berl).

1117   1998;136: 190–197. doi:10.1007/s002130050555

1118   111. Detke MJ, Rickels M, Lucki I. Active behaviors in the rat forced swimming test

1119   differentially produced by serotonergic and noradrenergic antidepressants.

1120   Psychopharmacology (Berl). 1995;121: 66–72. doi:10.1007/BF02245592

1121   112. Chen F, Larsen MB, Neubauer HA, Sanchez C, Plenge P, Wiborg O.

1122   Characterization of an allosteric citalopram-binding site at the serotonin

1123   transporter. J Neurochem. 2005;92: 21–28.

1124   doi:10.1111/j.1471-4159.2004.02835.x

1125   113. Bymaster F, Katner JS, Nelson DL, Hemrick-Luecke SK, Threlkeld PG,

1126   Heiligenstein JH, et al. Atomoxetine Increases Extracellular Levels of

1127   Norepinephrine and Dopamine in Prefrontal Cortex of Rat A Potential Mechanism

1128   for Efficacy in Attention Deficit/Hyperactivity Disorder.

1129   Neuropsychopharmacology. 2002;27: 699–711.
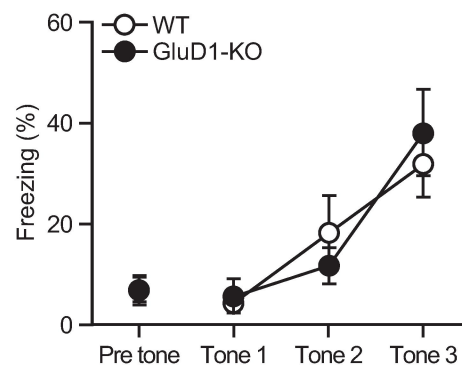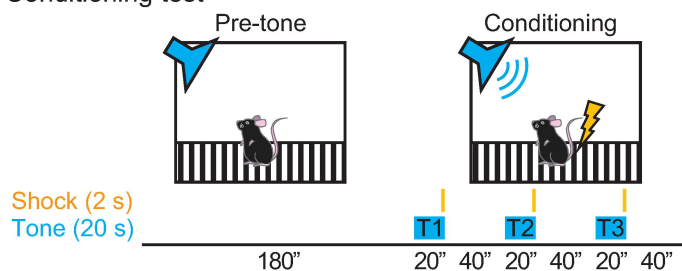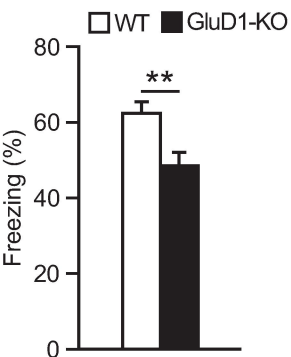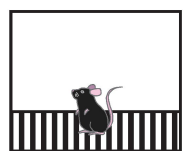
1130   doi:10.1016/S0893-133X(02)00346-9

1131

Figure 1

Figure 2

Resident-intruder test

Figure 3
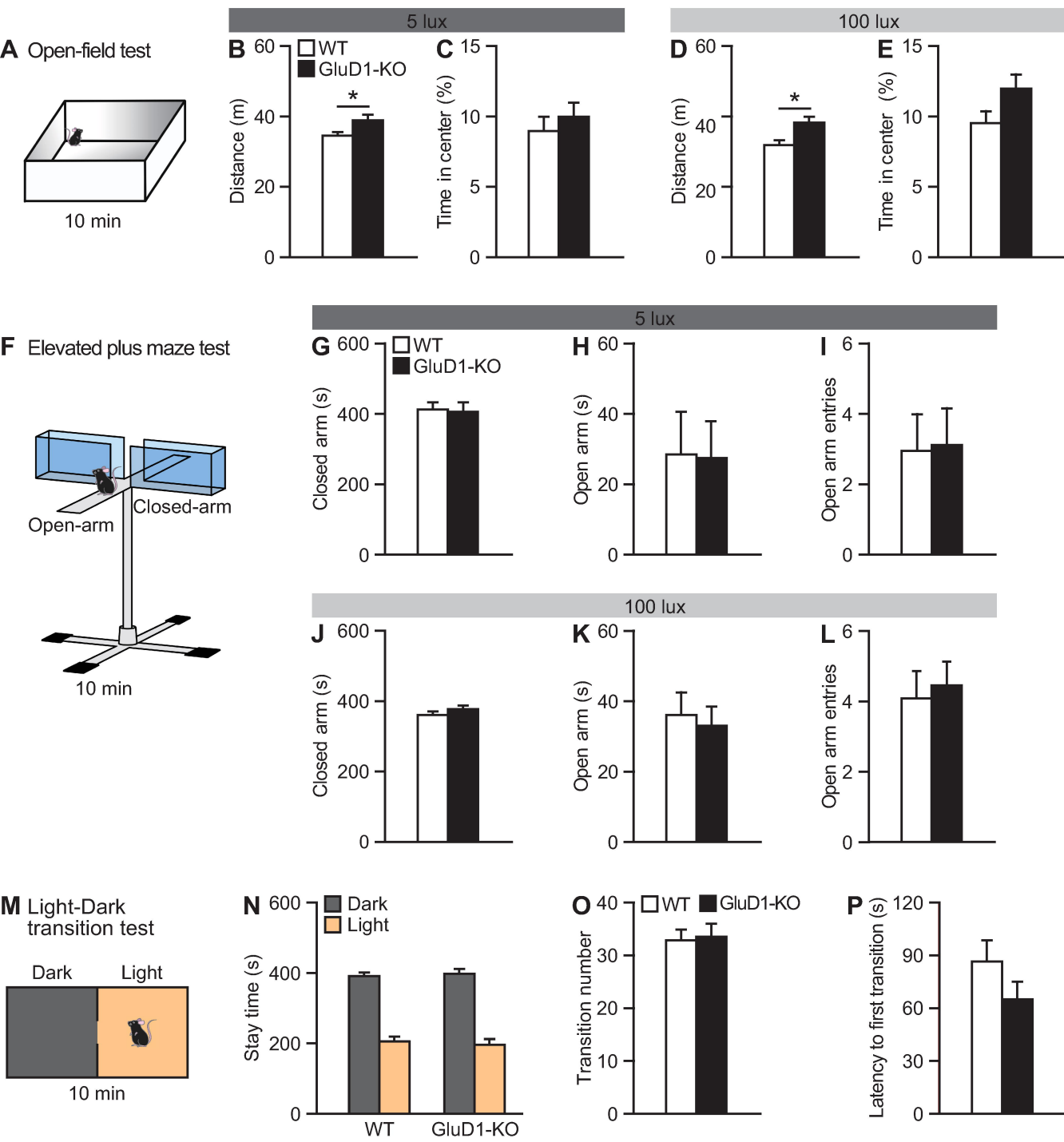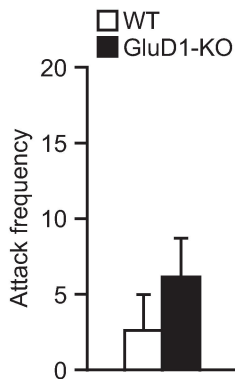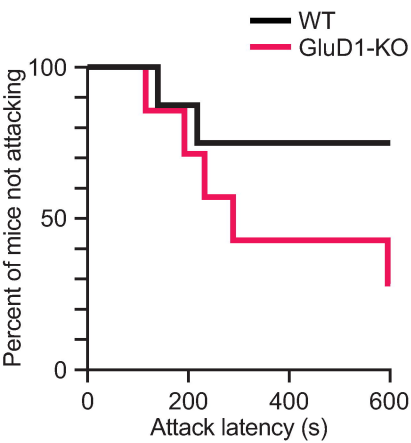
A Startle response

B Prepulse inhibition
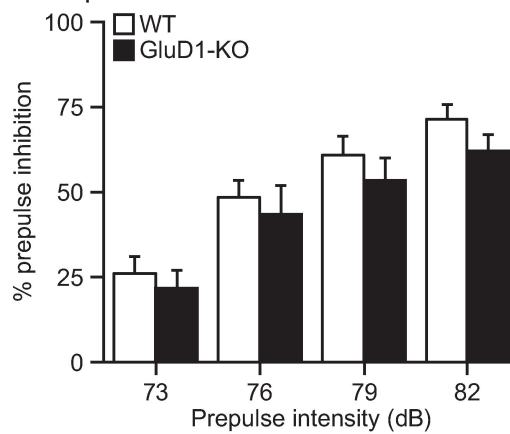
Figure 4

A Three-chambered social interaction test

Habituation
10 min

Stranger 1 · Empty

Sociability
10 min

Stranger 2 · Stranger 1

Social novelty preference
10 min

B Sociability

☐ WT ■ GluD1-KO

C Social novelty preference

Figure 5
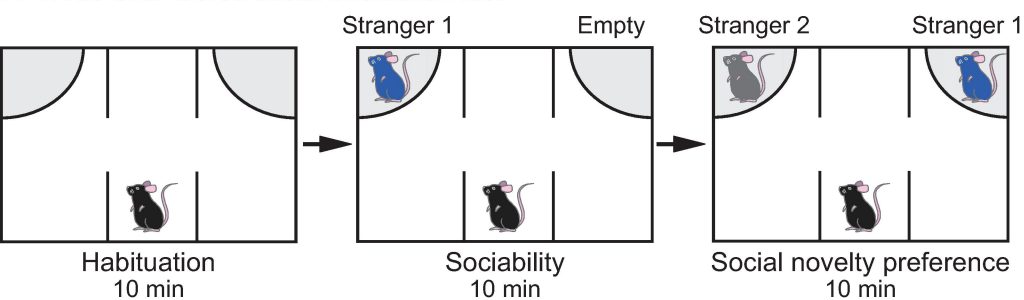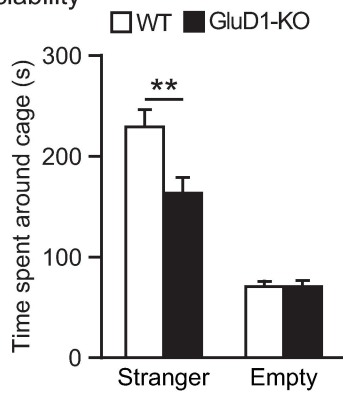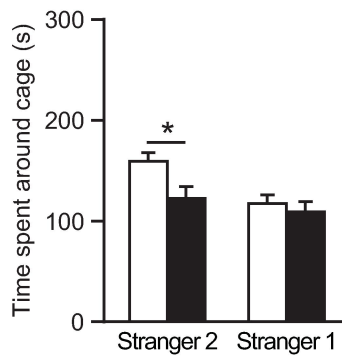
A Conditioning test

Shock (2 s)
Tone (20 s)

B Contextual test

C Cued test
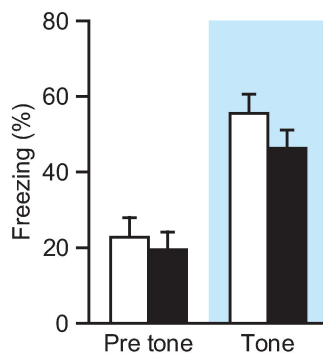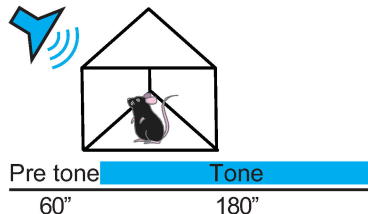
D Pain sensitivity

Figure 6

A Forced swim test

5 min

B Forced swim test with pharmacology

Drugs injection

60 min

Open-field test 10 min

5 min

Figure 7
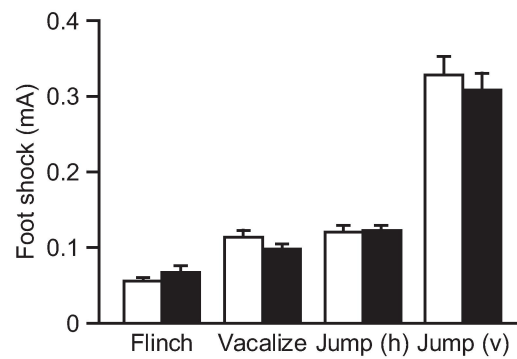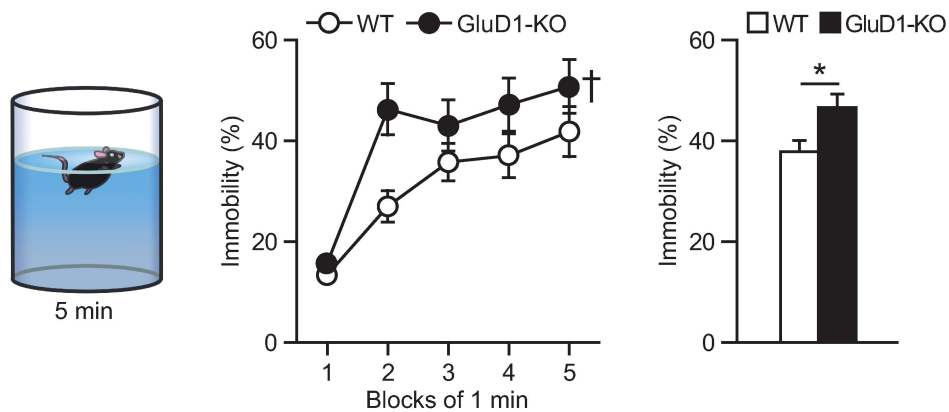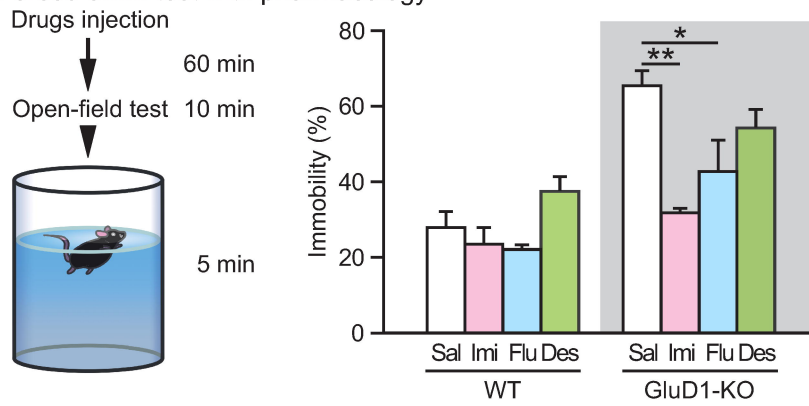
A Synaptosome fraction

B PSD fraction